

angular momentum and the parity of the 0.136-Mev excited level of Os^{186} . The comparative half-lives for the two beta-transitions to the ground and excited states of Os^{186} are of the same order of magnitude and hence must be of the same order of forbiddenness, involving probably the same spin change. This again suggests that the ground state of Re^{186} must have a spin 1. The same applies to the K -capture decay to the excited and ground states of W^{186} , which is also an *even-even* nucleus.

The extension of the one-particle spin-orbit coupling

model to odd-odd nuclei,¹⁰ also suggests a spin 1 and an odd parity for the ground state of Re^{186} , since the odd proton is presumably in a $d_{3/2}$ and the odd neutron in a $f_{7/2}$ state.⁸

The author wishes to express his thanks to Miss Phyllis Allen for performing the chemical separations and to Mr. Raymond R. McLeod for preparing the krypton-counter. He is also indebted to Dr. E. Bleuler for many discussions.

¹⁰ M. G. Mayer, *Phys. Rev.* **78**, 16 (1950).

Neutron Energy Distributions in Proton Bombardment of Be and C at 100 Mev*

DAVID BODANSKY† AND NORMAN F. RAMSEY
Nuclear Laboratory, Harvard University, Cambridge, Massachusetts
(Received March 1, 1951)

The energy distributions of neutrons emitted in the forward direction when beryllium and carbon targets are bombarded by 100-Mev protons were investigated. The neutron energy distribution was found from the range distribution of recoil protons from a polyethylene target, measured with a scintillation counter telescope. The distribution for beryllium was found to be peaked at about 93 Mev, while the distribution for carbon fell off rapidly above 70 Mev. The influence on the observed distribution of energy resolution effects, particularly those involving energy spread of the cyclotron proton beam, is discussed.

I. INTRODUCTION

AN investigation has been made of the energy distributions of the neutrons emitted in the forward direction when beryllium and carbon targets were bombarded by 100-Mev protons from the internal proton beam of the Harvard cyclotron. A collimated beam of the neutrons was allowed to fall upon two polyethylene scatterers. The recoil protons from one of these scatterers served as a monitor of the beam intensity while the range distribution of the recoil protons from the other scatterer was studied. From these results the energy distribution of the neutron beam was inferred.

II. DESCRIPTION OF EXPERIMENT

A diagram of the experimental arrangement is given in Fig. 1. The target was placed within the cyclotron tank at a location such that neutrons emitted in the forward direction with respect to the incident protons passed through a $\frac{1}{2}$ -inch thick Lucite window in the cyclotron vacuum tank and through a collimating hole in the 6-foot shielding surrounding the cyclotron.

The targets were rectangular bars $1\frac{3}{4}$ inches high, and, as held in the cyclotron, with a radial dimension of $\frac{1}{4}$ inch. The target was held by two light phosphor bronze clips which gripped the target at its top and bottom with small caps and which extended radially back from the target to a supporting probe. With this

arrangement the entire direct beam struck the target, and the contribution of scattered protons striking the holder was small. The beryllium target was 0.125 inch thick for all runs. Different carbon targets were used for runs A and B, 0.125 and 0.196 inch thick, respectively.

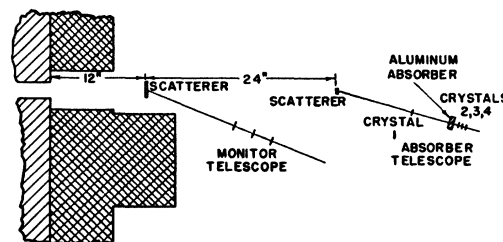
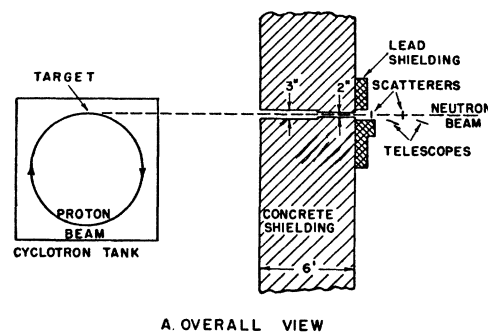


FIG. 1. Experimental arrangement.

* This work was partially supported by the joint program of the ONR and AEC.

† AEC Predoctoral Fellow. Now at Columbia University, New York, New York.

The collimated neutron beam fell upon two polyethylene scatterers. Scintillation counter telescopes, with 1P21 phototubes and anthracene crystals, were used to detect the resulting recoil protons. A monitor telescope viewed the first scatterer, and an absorber telescope viewed the second scatterer. The latter telescope was similar in principle to that first used with recoil protons by Van Allen and Ramsey¹ and subsequently used in similar experiments by many other observers. Arrangements quite similar to that in the present experiment were the ones used for neutron-proton scattering by Hadley² and Kelly *et al.*³ and for total cross sections of nuclei by Fox *et al.*⁴

The collinearity of the target, the axis of the collimating hole, and the centers of the scatterers were verified with the aid of a cathetometer and of plugs, with small centered holes, placed in the collimating hole. The center lines of the monitor and absorber telescopes made angles of 21 degrees and 15 degrees, respectively, with the axis of the collimating hole.

The monitor telescope used three scintillation counters

TABLE I. Dimensions of anthracene crystals.

Crystal	Distance from scatterer (cm)	Dimensions (cm)	Thickness (g/cm ²)
Monitor tel.			
1	27.3	2.64×2.60×0.44	0.54
2	33.6	3.42×1.98×0.43	0.54
3	40.0	3.74×2.12×0.41	0.52
Absorber tel.			
1	28.8	3.24×1.74×0.41	0.51
2	45.8	3.18×1.78×0.41	0.52
3	47.6	4.06×2.34×0.43	0.55
4	48.9	4.08×2.46×0.46	0.59

in triple coincidence. All the counting rates of the absorber telescope were normalized to the monitor telescope rate.

The absorber telescope consisted of four individual scintillation counters. Triple coincidences between counters 1, 2, and 3 (where increasing numbers correspond to increasing distance from the scatterer) and triple coincidences between counters 1, 2, and 4 were recorded simultaneously. In the geometry used the difference between the 1-2-3 and the 1-2-4 coincidence rates was due to the stopping power of the anthracene crystal associated with counter 3. This difference was therefore a measure of the number of particles from the polyethylene scatterer with sufficient energy to enter crystal 3 but insufficient energy to enter crystal 4. By interposing different thicknesses of aluminum absorber between counters 1 and 2, the energy interval thus

defined was increased from a lower limit imposed by the thickness of the first three crystals.

The measurement was repeated with a carbon scatterer and the polyethylene-carbon subtraction performed to obtain data for a differential range distribution of the recoil protons. From this the energy distribution of the incident neutrons was calculated.

Both polyethylene scatterers were $\frac{1}{4}$ inch thick. The monitor telescope scatterer was circular with a $2\frac{3}{4}$ -inch diameter. This was larger than the area of the incident neutron beam. The absorber telescope scatterer was rectangular with vertical and horizontal dimensions of $2\frac{1}{2}$ and $\frac{3}{4}$ inches, respectively. The carbon scatterer, used only with the absorber telescope, was of the same area and the same thickness, in carbon nuclei per cm², as the polyethylene scatterer.

Details of the telescope geometry are indicated in Table I. The anthracene crystals were obtained from the Harshaw Chemical Company. In the absorber telescope, where the thickness of wrapping and correct geometry were important, the crystals were wrapped in aluminum foil and centered using Lucite spacers between the crystals and phototubes.

The absorbers were placed between counters 1 and 2, as closely as possible to counter 2 to minimize scattering effects. They were 3 inches high, $1\frac{1}{2}$ inches wide, and of various thicknesses. 2s aluminum absorbers were used except for certain comparison tests in which lead absorbers were used.

In the absorber telescope, pulses from each counter were fed into Jordan-Bell amplifiers,⁵ which were modified to reduce overloading⁶ and dead-time effects. The amplifier discriminator outputs were fed into diode cut-off coincidence circuits and the coincidences counted with scalars. For the monitor telescope the amplifiers were replaced by two electron tubes for amplification and pulse shaping, which was ample in view of the large pulses obtained from scintillation counters.

Under typical conditions, with no absorbers, the observed counting rates were of the order of 600 monitor coincidences per minute, 200 absorber telescope coincidences per minute, and 5000 absorber telescope single-channel counts per minute.

III. TESTS OF EQUIPMENT

As recoil protons of different initial energies undergo different ionization losses in a given crystal, and therefore produce different size output pulses from the phototube, it was necessary to insure that the efficiency of the counting system was independent of the size of the phototube pulses over a reasonable range of sizes. This, and other features of proper telescope performance, were verified for both telescopes by obtaining triple coincidence plateaus with respect to phototube voltage, amplifier gain of each absorber telescope channel, and coincidence resolving time.

⁵ W. H. Jordan and P. R. Bell, *Rev. Sci. Instr.* **18**, 703 (1947).

⁶ W. G. Cross, *Phys. Rev.* **78**, 185 (1950).

¹ J. A. Van Allen and N. F. Ramsey, *Phys. Rev.* **57**, 1069 (1940).

² Hadley, Kelly, Leith, Segrè, Wiegand, and York, *Phys. Rev.* **75**, 351 (1949).

³ Kelly, Leith, Segrè, and Wiegand, *Phys. Rev.* **79**, 96 (1950).

⁴ Fox, Leith, Wouters, and MacKenzie, *Phys. Rev.* **80**, 23 (1950).

Counter 3 had the least transparent crystal and exhibited the poorest plateau with respect to amplifier gain. Its efficiency, for particles passing through it, was checked by simultaneous measurement of the 1-2-4 triple and 1-2-3-4 quadruple coincidence rates. At the gain which was used in the final runs, the 1-2-3-4 rate was 99 percent of the 1-2-4 rate. This discrepancy is attributed to possible failure to detect small pulses from counter 3, dead time losses, and an excess of accidental triple coincidences over accidental quadruple coincidences.

The over-all performance of the experimental arrangement was checked by a group of tests in which successively the cyclotron proton beam current was varied over a wide range, the target was removed, the collimating hole was plugged, the scatterer was moved off the axis of the hole, the scatterer thickness was varied, the anthracene crystal was removed from one phototube, the last counter of the telescope was moved out of line, and a thick absorber was placed in the telescope. No significant spurious effects were noted in any of these tests.

A difference between the 1-2-3 and 1-2-4 rates other than that due to the stopping power of crystal 3 would be uncovered by integral energy distribution curves. For a given absorber thickness the minimum energy which a proton must have for a 1-2-3 or 1-2-4 coincidence count is known. Figure 2 shows the 1-2-3 and 1-2-4 rates, after a polyethylene-carbon subtraction, as a function of minimum proton energy. The two sets of points appear randomly distributed about a mean curve, implying that there were no discrepancies between the two arising from faulty geometry.

IV. FACTORS DISTORTING ENERGY DISTRIBUTION

In addition to energy resolution effects, which will be discussed in the section on results, the observed energy distribution was distorted by attenuation of the neutron beam and scattering of the recoil protons. An order-of-magnitude calculation has been made which shows that these effects were not large enough to significantly alter the shape of the observed distributions, especially as the effects partially canceled each other.

The attenuation of the neutron beam in the target, the Lucite window of the cyclotron, and the polyethylene scatterers may be calculated from the total nuclear cross sections for neutrons at 42 Mev⁷ and 95 Mev.⁸ It is found, with the beryllium target, that the attenuation is 17 percent at 42 Mev and 8 percent at 95 Mev, causing a depression of the low energy end of the distribution with respect to the high energy end of about 10 percent.

The recoil protons from the polyethylene underwent coulomb and nuclear scattering in the absorbers, the greatest scattering, and therefore the greatest depression of the distribution, occurring at the high energy

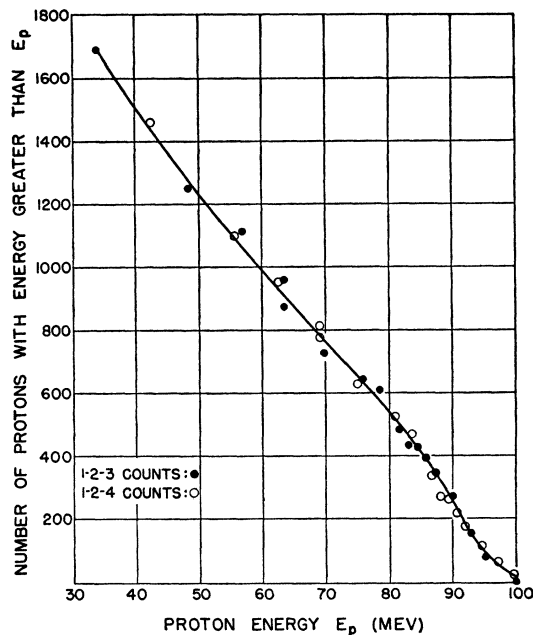


FIG. 2. Consistency test. Comparison of 1-2-3 and 1-2-4 coincidence counting rates.

end of the distribution where thick absorbers were used. This scattering has been investigated by an experimental method in which the location of the absorbers was changed. In the absorber telescope the crystals of counters 1 and 2 were 17 cm apart. Normally, the absorber was placed as closely as possible to counter 2 to minimize the effects of scattering. On moving the absorber back from counter 2 towards counter 1, the solid angle subtended by counter 2, as seen by the absorber, decreases. The resulting decrease in counting rate can be used to estimate part of the scattering loss which occurred when the absorber was in its normal position.

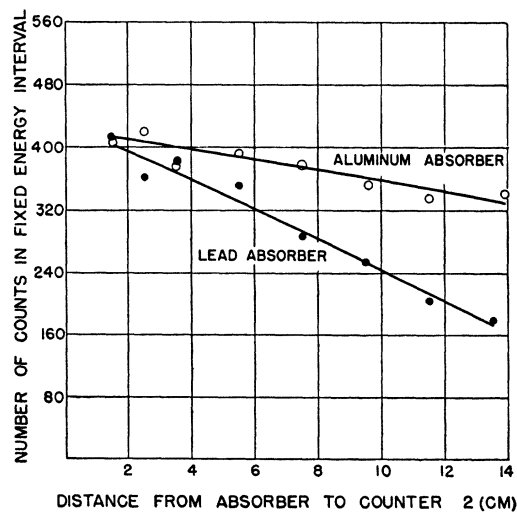


FIG. 3. Effect of scattering of recoil protons in the absorbers.

⁷ R. H. Hildebrand and C. E. Leith, *Phys. Rev.* **80**, 842 (1950).

⁸ J. DeJuren and N. Knable, *Phys. Rev.* **77**, 606 (1950).

The results of such a measurement with aluminum and lead absorbers are given in Fig. 3 for recoil protons stopped in counter 3. In each case an absorber thickness was chosen such that the average energy of the protons stopping in counter 3 was about 70 Mev. The width of the interval in initial energies of protons stopping in counter 3 is greater with lead absorbers than with aluminum absorbers. (This seemingly paradoxical result arises from the energy dependence of the relative stopping powers of different materials.) The observed counting rates for lead have been corrected to equalize the width of these intervals.

It is seen from Fig. 3 that the scattering effects are greater for the lead than for the aluminum absorbers. It is estimated by extrapolation that with the $\frac{1}{2}$ -inch aluminum absorber in its normal position the scattering loss was about 3 percent. It is calculated from this

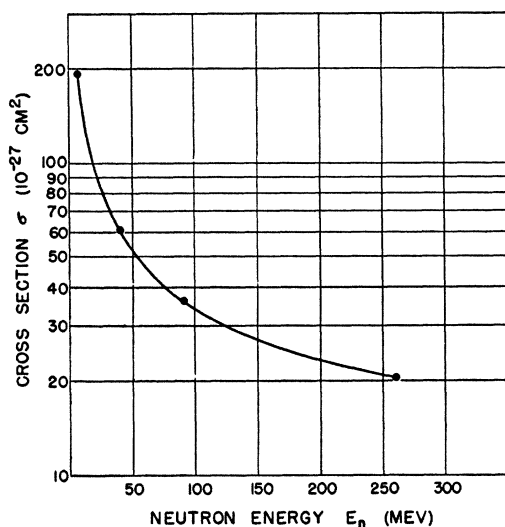


FIG. 4. Assumed neutron-proton scattering cross section σ for the scattering of recoil protons into an angle of 15 degrees in the laboratory system (per unit solid angle).

result, using a $1/E$ energy dependence of scattering, that the loss was about 5 percent at the high energy end of the distribution.

For this method to be valid, the fraction of scattered protons which were detected must vary appreciably with absorber position. A consideration of the telescope geometry and scattering angles indicates that this requirement was satisfied for the multiple coulomb scattering. Adequate information on nuclear scattering of protons by nuclei is not available. Assuming that the qualitative features of the nuclear scattering of protons by nuclei are similar to those of the scattering of neutrons by nuclei, it is concluded from neutron scattering results at 84 Mev⁹ that (a) the experimental method estimated the effect of elastic nuclear scattering, (b) few of the inelastically scattered protons were detected by

⁹ Bratenahl, Fernbach, Hildebrand, Leith, and Moyer, Phys. Rev. **77**, 597 (1950).

the telescope in any absorber position and therefore the experimental method did not measure the inelastic scattering loss, and (c) the loss at the high energy end of the distribution due to inelastic nuclear scattering was about 10 percent, as calculated from the inelastic cross section for neutrons.

On this basis, which can only indicate orders of magnitude, the total loss due to scattering in the thickest absorbers was about 15 percent. This loss was partly compensated for, in the energy distribution results, by the attenuation of the neutron beam. Considerably larger distortions than this would be required to change the main features of the observed energy distributions.

V. CALCULATIONS

To find the energy distribution of the neutron beam, different thicknesses of absorber were placed in the absorber telescope. For each thickness the normalized 1-2-3 and 1-2-4 rates were obtained with a polyethylene scatterer and with a carbon scatterer. As the carbon scatterer was chosen to have the same number of carbon nuclei per cm^2 as the polyethylene, a direct subtraction gives the number of recoil protons from the hydrogen atoms in the polyethylene. (The error introduced due to the different stopping power of the two scatterers is small.) Background counts are subtracted out in the carbon subtraction. The difference between the 1-2-3 and 1-2-4 rates gives the number of protons within a particular range interval.

The proton energy, E_p , associated with a proton range was calculated using the Bethe-Bloch ionization loss formula. Previously calculated tables¹⁰ and graphs¹¹ were employed both directly where applicable and by use of the relative stopping powers of the substances involved in the other cases. The mean ionization potentials were taken as: air, 80.5 ev; aluminum, 150 ev; carbon, 69 ev; hydrogen, 17.5 ev; lead, 943 ev.

The corresponding neutron energy, E_n , was calculated from the approximate two-body collision equation,

$$E_n = E_p \sec^2 \theta (1 + E_p \tan^2 \theta / 2Mc^2),$$

where θ is the angle of the recoil proton in the laboratory system and Mc^2 is the rest energy of a nucleon.

In calculating the number of neutrons per unit energy interval corrections were made for the energy dependence of the neutron-proton scattering cross section and for the energy dependence of the width of the energy intervals defined by the crystal of counter 3.

The energy dependence of the scattering is not known in detail, but data is available which allows a reasonable interpolation. The scattering cross section per unit solid angle, σ , for recoil protons at an angle of 15 degrees in the laboratory system is tabulated in measurements at 40 Mev,² 90 Mev² and 260 Mev.³ It can be calculated from a measurement at 14 Mev¹² assuming

¹⁰ J. H. Smith, Phys. Rev. **71**, 32 (1947).

¹¹ Prepared by E. P. Gross, Princeton University (1947).

¹² H. H. Barshall and R. F. Taschek, Phys. Rev. **75**, 1819 (1949).

spherical symmetry in the center-of-mass system. These values are plotted in Fig. 4 and a smooth curve used to interpolate for values of σ at intermediate energies. The errors introduced by this method are limited by the fact that the values at 40 and 90 Mev correspond closely to the extent of the region of interest of this experiment.

The energy interval defined by the crystal of counter 3 decreases in width, from about 9 Mev to 4 Mev, as thicker absorbers are used and higher energy protons counted. To obtain the number of protons per unit energy interval, one divides the observed counting rate by the width of the interval, or, equivalently for narrow intervals, by the rate of ionization energy loss, dE/dx (in Mev per g/cm²), evaluated at the initial energy of the recoil proton. Except for a small relativistic term the width of the neutron energy interval is proportional to the width of the proton energy interval.

The relative neutron energy distribution was obtained by multiplying the observed range distribution by $1.69 \times 10^{-25} / [\sigma(E_n)(dE/dx)_{E_p}]$, where an arbitrary multiplicative factor has been included. No corrections have been made for the distortion effects discussed in Sec. IV.

VI. RESULTS

The results of three runs with a beryllium target, and two runs with a carbon target are shown in Figs. 5 and 6. Between the time that runs A were taken and runs B were taken, the absorber telescope was dismantled and changes were made in the cyclotron oscillator and target probe systems. It was not expected that these changes would alter the observed distributions. However, there is a clear discrepancy between the A runs and the B runs.

The qualitative features of the results are not affected by these discrepancies. It is to be noted that there is a peak in the neutron energy distribution from beryllium at about 93 Mev, while the carbon distribution falls off rapidly above 70 Mev.

The relative normalization for the beryllium and carbon targets is significant only as to orders of magnitude. The relative normalization is based on run B, in which the beryllium and carbon targets were held on a single probe, and alternated, by rotation of the probe, to provide measurements with the same cyclotron beam current. Targets of the same thickness in nuclei per cm² were used in run B; but owing to the greater rms angle of multiple scattering in the carbon, it is believed that there were fewer multiple traversals and therefore a smaller effective beam current for the carbon target.¹³

The stable orbit energy of the cyclotron protons, as calculated from the target radius and magnetic field, was approximately 116 Mev. The actual energy distribution of the protons incident upon the beryllium target has been measured by Bloembergen and Van

¹³ See W. J. Knox, Phys. Rev. **81**, 693 (1951), for a study of the relation between target thickness and effective beam current.

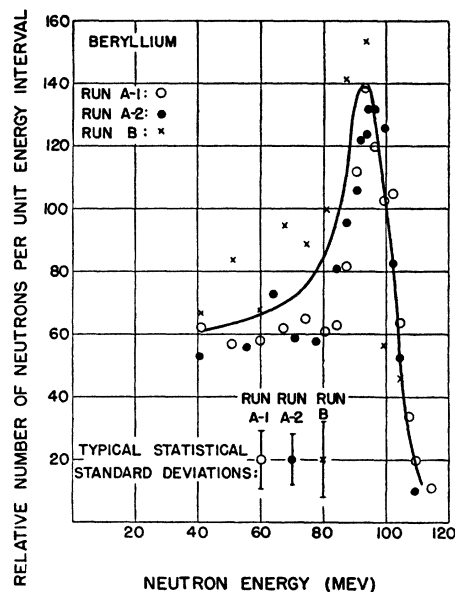


FIG. 5. Energy distribution of neutrons from beryllium target bombarded by 100-Mev protons.

Heerden using a method in which protons scattered from the target are focused by the cyclotron magnetic field and detected by photographic plates.¹⁴ They found the incident proton distribution of Fig. 7 which is similar in shape and width to the neutron energy distribution for beryllium of Fig. 5. The wide distribution of incident proton energies is believed due to oscillations of the circulating proton beam and to multiple traversals of the target. The proton distribution with

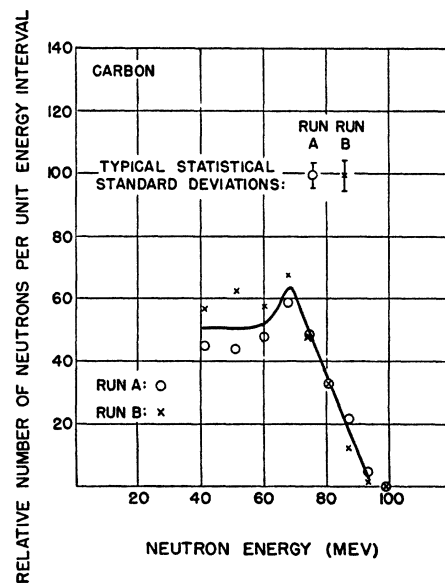


FIG. 6. Energy distribution of neutrons from carbon target bombarded by 100-Mev protons.

¹⁴ N. Bloembergen and P. J. Van Heerden, Phys. Rev. (to be published) and further work to be published.

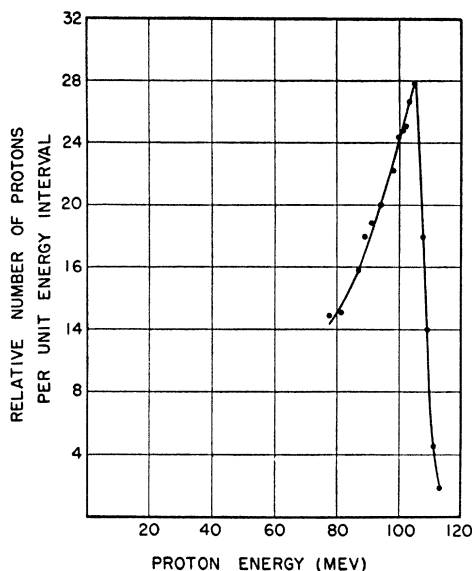


Fig. 7. Energy distribution of protons incident upon beryllium target.

the two carbon targets is believed, from considerations of the target thicknesses, to have not been significantly different from that of Fig. 7.

The wide proton beam energy distribution overshadows other energy resolution effects such as energy

loss and coulomb scattering of the recoil protons in the polyethylene scatterer, limited angular resolution in the counting telescopes, and straggling in the absorbers. These effects would introduce a half-width of about 7 Mev and a lowering of the position of the peak by about 3 Mev were the neutron beam from the beryllium target monoenergetic. In the present case they increase the width of the observed peak by only about 1 Mev but still lower the energies by about 3 Mev.

Comparison of Figs. 5 and 7 indicates that the peak of the neutron energy distribution from beryllium is about 10 Mev below the peak of the energy distribution of the incident protons and that a considerable portion of the width of the neutron energy distribution curve is due to the spread in energy of the incident protons. A further comparison with Fig. 7 indicates a much lower mean energy for the neutrons from carbon than for those from beryllium.

We are indebted to J. A. Hofmann for his assistance in much of this work. We wish to express our gratitude to the staff of the Harvard Nuclear Laboratory for their help and particularly to A. C. Grant and the cyclotron operating crew for the many hours contributed to the experiment. Thanks are due R. W. Birge, W. G. Cross, N. M. Hintz, and L. S. Lavatelli for their suggestions and aid, and to N. Bloembergen for the measurement of the proton beam energy.

Interaction of Mesons with Nuclei

SATIO HAYAKAWA*

Laboratory of Nuclear Science and Engineering, Massachusetts Institute of Technology, Cambridge, Massachusetts

(Received October 9, 1950)

The interaction of slow π -mesons with nuclei is treated phenomenologically. A nucleus is assumed to be a continuum with potential with respect to a meson. The potential consists of real and imaginary parts, corresponding to the polarization caused by a meson and the absorption of a meson, respectively. The scattering, the absorption, and the production of mesons are qualitatively discussed by analogy with the current theory of nuclear reactions. The difference from the theory based on the weak interaction of mesons with nucleons is presented.

I. INTRODUCTION

ALTHOUGH the qualitative nature of mesons is clear, there are serious difficulties in deducing quantitative information about their nature from experiments. These difficulties arise from the small amount of experimental data available and from the inadequacy of their interpretation by current meson theories. In most experiments we can observe the interaction of mesons with nuclei but not with nucleons, whereas meson theory is related most simply to the interaction of mesons with individual nucleons. There have been several works in which the effect of nuclear binding is

taken into account.¹⁻³ These works, however, start from the interaction between a meson and a nucleon, and the effect of nuclear binding is considered afterwards in such a way that the nucleons obey some momentum distribution law and the Pauli principle. Furthermore, it is assumed that a meson does not interact with any nucleon after it is produced or before it is

¹ Fujimoto, Nishijima, Okabayashi, Takayanagi, and Yamaguchi, *Prog. Theor. Phys.* **5**, 870 (1950).

² Fujimoto, Takayanagi, and Yamaguchi, *Prog. Theor. Phys.* **5**, 498 (1950).

³ M. Lax and H. Feshbach, *Phys. Rev.* **81**, 189 (1951). This gives good agreement with experiments for the production of charged mesons, but for the production of neutral mesons a certain modification is required.

* On leave from Osaka City University, Osaka, Japan.